UC Irvine
UC Irvine Previously Published Works

Title
Long-range transport of sulfur dioxide in the central Pacific

Permalink
https://escholarship.org/uc/item/14h36417

Journal
Journal of Geophysical Research, 109(D15)

ISSN
0148-0227

Authors
Tu, Fang Huang
Thornton, Donald C
Bandy, Alan R
et al.

Publication Date
2004

DOI
10.1029/2003jd004309

Copyright Information

Peer reviewed

Long-range transport of sulfur dioxide in the central Pacific

Fang Huang Tu,[1] Donald C. Thornton,[1] Alan R. Bandy,[1] Gregory R. Carmichael,[2] Youhua Tang,[2] K. Lee Thornhill,[3] Glenn W. Sachse,[3] and Donald R. Blake[4]

[1]   Long-range transport of sulfur dioxide (SO_2) from east Asia to the central North Pacific troposphere was observed on transit flights during the NASA Transport and Chemical Evolution over the Pacific mission. A series of SO_2-enhanced layers above the boundary layer was observed during these flights. The significant features included enhanced SO_2 layers associated with low water vapor and low turbulence that were usually dynamically isolated from the marine boundary layer. This study shows that atmospheric dynamics were very important in determining the SO_2 distributions in the central Pacific during March and April 2001. Trajectory studies revealed that SO_2-enhanced layers could be connected to both volcanic and anthropogenic sources in east Asia. These trajectory studies also showed that the air parcels usually were lifted 2 km above the source regions and then progressed to the east in the midlatitudes ($30°-60°N$). The air parcels arrived in the central Pacific within $2-3$ days. Sulfur dioxide transported at altitudes of $2-4$ km dominated the SO_2 distribution in the central Pacific. A comparison of SO_2 observations and results of chemical transport models indicated that SO_2 was removed primarily by cloud processes. Therefore, in the absence of cloud, SO_2 can be transported long distances if the trajectory is decoupled from the boundary layer. Another important observation was that the Miyake-jima volcano made a major contribution to the SO_2 concentrations in the central Pacific troposphere during March and April 2001. At times, the volcanic SO_2 had more influence in the central Pacific than the six largest anthropogenic SO_2 source regions in east Asia.   *INDEX TERMS:* 0322 Atmospheric Composition and Structure: Constituent sources and sinks; 0365 Atmospheric Composition and Structure: Troposphere—composition and chemistry; 0368 Atmospheric Composition and Structure: Troposphere—constituent transport and chemistry; 0370 Atmospheric Composition and Structure: Volcanic effects (8409); *KEYWORDS:* sulfur dioxide, long-range transport, North Pacific

1.   Introduction

[2]   The growing economic activity and the anthropogenic emissions in eastern Asia have raised major questions concerning how anthropogenic emissions impact the Pacific atmosphere. Many instances of long-range transport of gases and aerosols to the Pacific have been reported [*Andreae et al.*, 1988; *Bailey et al.*, 2000; *Clarke et al.*, 2001; *Duce et al.*, 1980; *Harris et al.*, 1992; *Hoell et al.*, 1997; *Jaffe et al.*, 1999, 2003a, 2003b; *Martin et al.*, 2002; *Merrill et al.*, 1989; *Moore et al.*, 2003; *Perry et al.*, 1999; *Prospero and Savoie*, 2003; *Shaw*, 1980; *Steding and Flegal*, 2002]. Long-range transport of gases and aerosols

from east Asia to the Pacific have been most intense during springtime [*Duce et al.*, 1980; *Jaffe et al.*, 2003a, 2003b; *Martin et al.*, 2002; *Moore et al.*, 2003; *Prospero and Savoie*, 2003] because of strong midlatitude westerly winds during this season [*Bey et al.*, 2001; *Wilkening et al.*, 2000; *Xiao et al.*, 1997]. *Merrill et al.* [1989] showed that the Asian dust concentrations in the North Pacific had an broad annual maximum during February to May. *Prospero and Savoie* [2003] showed that the non-sea-salt sulfate, nitrate, mineral dust, and methanesulfonate (MSA) concentrations had similar annual maxima in the months of March to May at Midway Island ($28.2°N$ $177.4°W$). Studies by *Andreae et al.* [1988] on the west coast of Washington State suggested that the air masses arriving there were from east Asia and had been over the Pacific for $4-8$ days. Observations by *Jaffe et al.* [1999] at Cheeka Peak Observatory in Washington State during March–April 1997 indicated that the surface emissions from Asia were lifted into the free troposphere over Asia and then transported to North America in ~6 days.

[3]   The mechanisms for the transport of SO_2 from its sources in east Asia across the Pacific and its impact on the

---

[1]Department of Chemistry, Drexel University, Philadelphia, Pennsylvania, USA.

[2]Center for Global and Regional Environmental Research, University of Iowa, Iowa City, Iowa, USA.

[3]NASA Langley Research Center, Hampton, Virginia, USA.

[4]Department of Chemistry, University of California, Irvine, California, USA.

Pacific troposphere have not been fully resolved. Sulfur dioxide plays an important role in the atmospheric sulfur cycle through its role in the formation of new aerosols and the modification of existing aerosols. The rapid growth in fossil fuel usage in Asia during the 1980s, especially the increase in the use of high sulfur coal for fuel, has raised concerns about the potential impact of SO$_2$ on the western Pacific troposphere in particular and on global climate in general. These concerns increased when *Thornton et al.* [1996, 1997] directly observed during NASA (Pacific Exploratory Mission) PEM West A and B missions that SO$_2$ was being transported from sources in east Asia to the atmosphere of western Pacific.

[4] The work reported here is a further investigation of the transport of SO$_2$ from east Asian sources to the atmosphere of the North Pacific. It is based on data obtained during the NASA Transport and Chemical Evolution over the Pacific (TRACE-P) mission. That mission was flown in 24 February to 10 April 2001. The TRACE-P was designed to study the transport and evolution of anthropogenic chemical species in the North Pacific troposphere [*Jacob et al.*, 2003]. Unlike previous GTE missions in which SO$_2$ data were obtained with a frequency of one sample every 5 min, TRACE-P SO$_2$ data were obtained at a frequency of 25 measurements per second with an new type of atmospheric pressure ionization mass spectrometer [*Thornton et al.*, 2002]. This high-frequency data provided a view of the dynamics of SO$_2$ transport that was previously impossible and has led to a much better understanding of the importance of atmosphere dynamics in controlling the transport and distribution of SO$_2$.

2. Experimental Procedure

[5] Sulfur dioxide was determined by an atmospheric pressure ionization mass spectrometer using isotopically labeled standard (APIMS/ILS) and was deployed on the NASA Wallops P-3B aircraft during TRACE-P. This instrument was described in detail by *Thornton et al.* [2002] and will be described only briefly in this paper.

[6] This instrument was based on a quadrupole mass spectrometer and used an atmospheric pressure ^{63}Ni source in which SO$_2$ was ionized by reactions with other ions formed in the source. ^{34}SO$_2$ was added as an internal standard to ambient air near the inlet of the manifold [*Bandy et al.*, 1993]. The ion chemistry and declustering region produced SO$_5^-$ ions that were monitored alternately at mass/charge (m/e) 112 for the ambient signal and m/e 114 for the labeled standard. The count rate for each ion was integrated for 20 ms, and the ambient SO$_2$ concentration was computed every 40 ms (25 Hz sampling rate). Data processing accounted for the isotopic abundances in ambient air and in the standard as previously described by *Bandy et al.* [1993]. Blank corrections were made using data for SO$_2$ free air [*Thornton et al.*, 2002] and ambient air without the standard added. The 25 Hz data were averaged to 1-s data for the TRACE-P archive.

[7] The lower limit of detection for a 10-s integration time was 1 pptv. The precision was 3 pptv for a 1-s integration time for SO$_2$ concentrations below 100 pptv and <2% above 100 pptv. The accuracy was 5% based on the calibration of the 153 ppbv ^{34}SO$_2$ standard (Scott-

Marrin, Inc., Riverside, California) which, in turn, was calibrated against three ^{32}SO$_2$ permeation tubes (VICI Metronics, Poulsbo, Washington). The permeation tubes were gravimetrically calibrated.

[8] The turbulent air motion measurement system (TAMMS) [*Thornhill et al.*, 2003] provided 25 Hz data for the *u*, *v*, *w* components of the wind, water vapor mixing ratio (MR) from a Lyman α absorption sensor, static temperature, and pressure. The SO$_2$ counts data were recorded by the TAMMS data system to insure that the time recorded for the SO$_2$ counts would be identical to the time recorded for the three component wind data. Additional meteorological data were provided by the GTE project for the P-3B (TRACE-P data archive).

[9] The archived 5-day back trajectories for the TRACE-P mission (http://www-gte.larc.nasa.gov/trace/TP_dat.htm) were used to identify the origins and the pathways of the air parcels intercepted in TRACE-P. These trajectories were calculated using a kinematic model employing the *u*, *v*, and *w* wind components from the ECMWF analyses reported by *Fuelberg et al.* [2003]. A cubic spline procedure was used to vertically interpolate the gridded data from the 61 initial sigma levels to 191 constant pressure levels at 5-hPa intervals between 1000 and 50 hPa. Linear interpolation provided values within these 5-hPa intervals and at the parcel's precise horizontal locations. Linear interpolation was also used to temporally interpolate at 5-min time steps. Additional details about the trajectory model, along with a comparison between kinematic and isentropic trajectories, are given by *Fuelberg et al.* [1996].

[10] In this work, the NOAA Hybrid Single-Particle Lagrangian Integrated Trajectory (HYSPLIT) model was used to generate the trajectories and simulate the SO$_2$ distributions in the central Pacific. HYSPLIT is a model for computing trajectories, complex dispersion, and deposition using puff or particle approaches [*Draxler and Hess*, 1997, 1998]; also see http://www.arl.noaa.gov/ready/hysplit4.html). All HYSPLIT model results were based on the NOAA Air Resources Laboratory final (FNL) data set.

3. Results and Discussion
3.1. Observations During TRACE-P Transit Flights

[11] A series of SO$_2$-enhanced layers in the North Pacific were encountered during the TRACE-P transit flights (Figure 1). The transit flights were flown with a stair step pattern across the North Pacific (Figure 1b). One of the most important features observed during these flights was that the SO$_2$-enhanced layers were usually encountered between the top of the marine convective boundary layer (CBL) and 5 km.

[12] The most striking feature observed during these transit flights was the highly structured atmospheric profiles obtained near Midway Island (28.2°N 177.4°W). An important aspect was that these SO$_2$-enhanced layers usually were observed just above the CBL. In flight 20, a SO$_2$ layer at 31.5°N 174.7°E (Figure 2a) was observed just above the CBL. At the beginning of flight 21, SO$_2$-enhanced layers near 26.5°N 179.2°E (Figure 3a) were also observed just above the CBL.
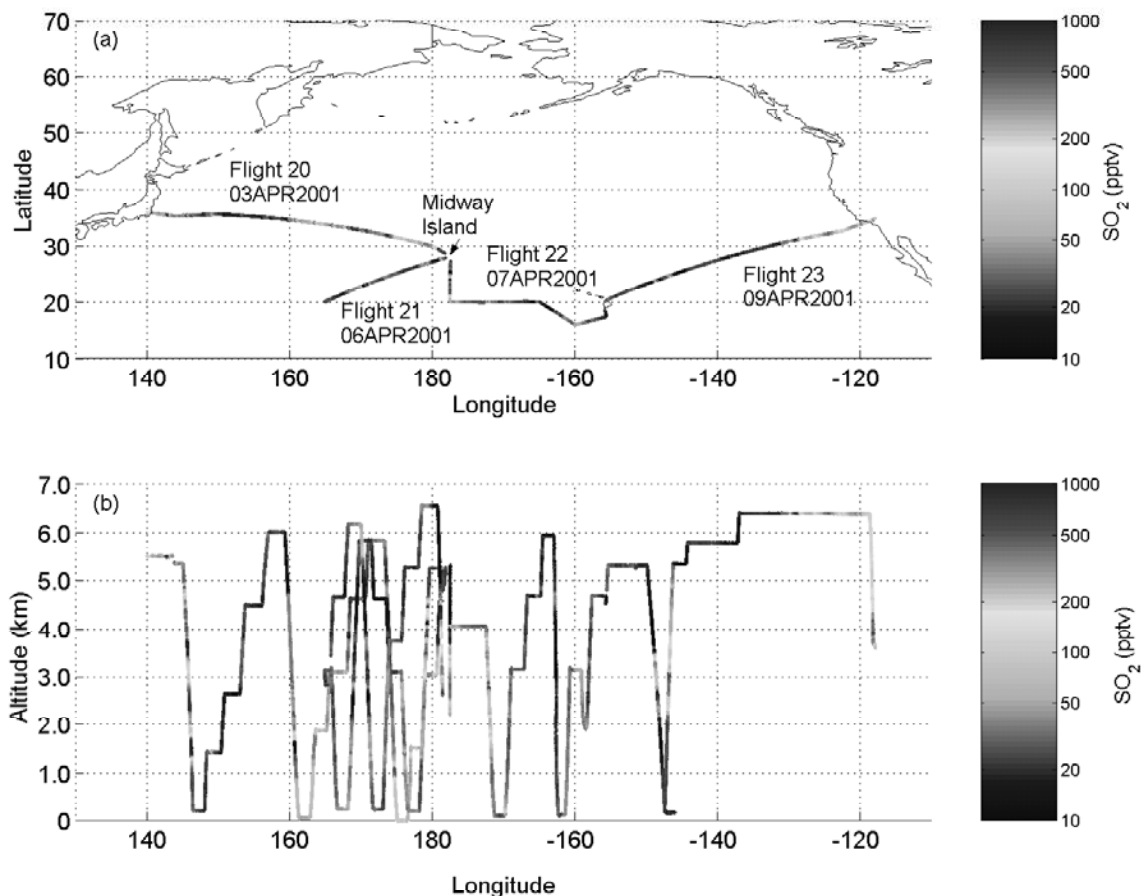
Figure 1. The SO$_2$ distributions along the trans-Pacific flight tracks during TRACE-P: (a) flight tracks and (b) altitude profiles. Note the highly varied SO$_2$ concentrations near Midway Island between 1 and 5 km. See color version of this figure at back of this issue.

[13] The second important feature was that an air mass was apparently intercepted on two flights on consecutive days. On P3-B flight 21, the SO$_2$ concentrations were mainly below 100 pptv along the flight track southwest of Midway Island. At the end of flight 21 near Midway Island at 27.7°N 178.8°W, a vertical profile between 2.5 and 4.7 km revealed a layer containing about 1.3 ppbv of SO$_2$ (Figure 4a). These profiles had similar chemical signatures as those profiles observed at the beginning of flight 21 (Figure 3). On flight 22, SO$_2$-enhanced layers (Figure 5a) were observed near 24.5°N 177.5°W. The profiles observed at this location had similar atmospheric chemical signatures to those observed in flight 21. The wind directions were mainly west to northwest for these profiles. The streamlines at 700 and 500 hPa were mainly from northwest to southeast. The wind directions and streamlines suggested that the same air masses were repeatedly encountered near Midway Island.

[14] There were no major SO$_2$ sources in the western central Pacific in spring 2001. However, over 1 ppbv of SO$_2$ appeared in regions normally thought to be pristine. Similar vertical profiles were repeatedly observed along the wind streamlines during flights 21 and 22. These observations suggest that the SO$_2$ in the central Pacific resulted from long-range transport from the major sources in other regions.

3.2. SO$_2$ Transport Routes: Trajectory Studies

[15] Typical 5-day back trajectories from the TRACE-P data archives for SO$_2$-enhanced layers during transit flights are shown in Figure 6. Each solid symbol represents a 1-day interval. The back trajectories indicate that the enhanced SO$_2$ layers originated from east Asia, which is known to have significant SO$_2$ source regions [Streets et al., 2003]. In general, the trajectories indicated that the air parcels from east Asia followed two different routes toward the central Pacific: an eastern route and a northeastern route. On the eastern route, the air parcels moved eastward toward the central Pacific on trajectories between 30° and 40°N. On the northeastern route, the air parcels moved northeastward on trajectories between 40° and 60°N and circled to the southeast toward the central Pacific or toward the eastern Pacific. Typically, the air parcels initially were lifted above 3 km while they continued moving in either the eastern or the northeastern route.

[16] The predominantly eastward trajectories (solid lines in Figure 6) usually subsided to lower altitudes in the western Pacific and had less chance to arrive in the central
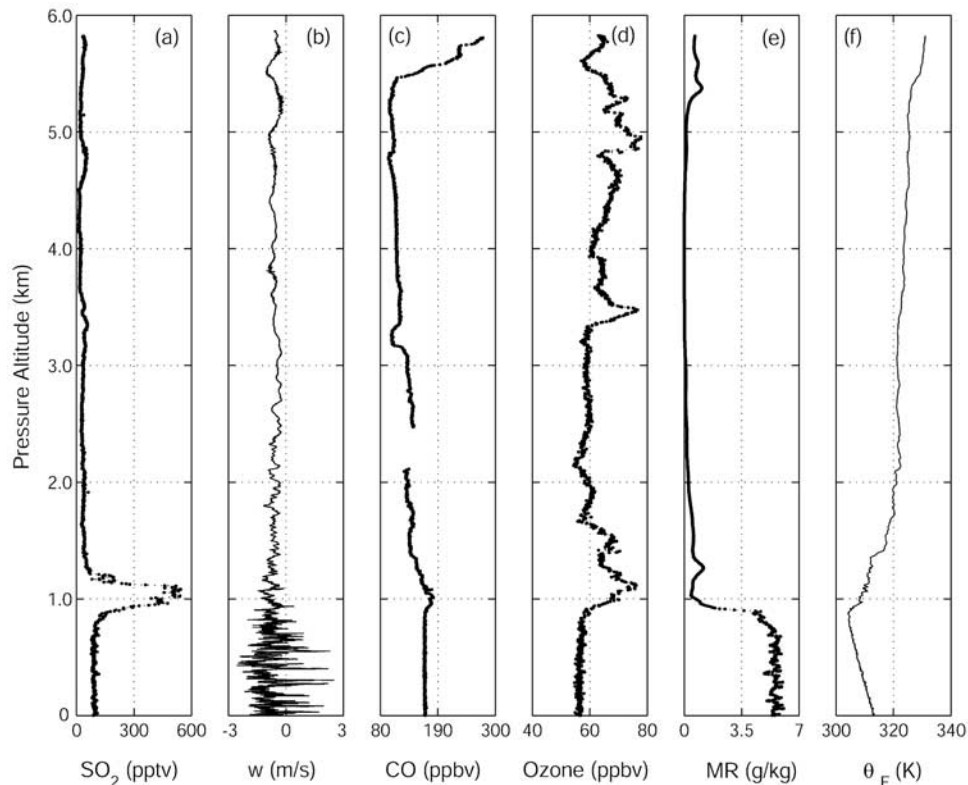
Figure 2. Vertical descent profiles of (a) SO$_2$, (b) vertical wind velocity (w) indicating turbulence, (c) CO, (d) O$_3$, (e) water vapor mixing ratio (MR), and (f) equivalent potential temperature (θ_E) near 31.5°N 174.7°E during flight 20. Data are 1 Hz except for 10 Hz w. Note the enhanced SO$_2$ and O$_3$ in a dry layer just above the convective boundary layer (CBL) top (900 m). The slow entrainment process and rapid loss SO$_2$ to the ocean surface and aerosols limited the SO$_2$ concentrations in the CBL.

Pacific without loss to the CBL. The northeast trajectories (dashed lines in Figure 6) usually stayed at higher altitudes and reached the central and eastern Pacific within 3 days. Depending on the atmospheric conditions, the air parcels could move farther east or subside to lower altitudes. The subsiding air parcels are expected to have low absolute humidity.

3.3. Atmospheric Chemical Signatures

[17] A defining feature of the lower troposphere observed in central Pacific during TRACE-P was the complexity of its chemistry and meteorology, which was made visible by the high-frequency data. Vertical profiles obtained during flight 20 at 31.5°N 174.7°E (Figure 2) had enhanced SO$_2$ and O$_3$ just above the CBL. The peak SO$_2$ concentration was about 540 pptv at 1.1 km. This layer was characterized by its low turbulence (less than ±0.5 m/s, Figure 2b) and low water vapor concentration (less than 0.5 g/kg, Figure 2e).

[18] Inspection of the back trajectories in this location (Figure 6, solid line with circles) suggested that this SO$_2$ and O$_3$ enhanced layer came from northeast China. The air parcels were apparently lifted to the mid-troposphere and then subsequently compressed into thin layers by subsidence. The low-turbulence conditions limited the vertical mixing of the SO$_2$.

[19] The CBL top was about 0.9 km as indicated by the sharp change in the water vapor mixing ratio (MR) (4.6 g/kg to 0.4 g/kg, Figure 2e). In the CBL, the substantial turbu-

lence and the almost constant concentrations of SO$_2$, carbon monoxide (CO), O$_3$, and water vapor indicated that the CBL was well mixed.

[20] Away from sources, the ratio of ethyne (C$_2$H$_2$) to CO is known to decrease with time and it is often used as an indication of the age of an anthropogenic plume [*McKeen and Liu*, 1993; *McKeen et al.*, 1996; *Sandholm et al.*, 1992, 1994; *Smyth et al.*, 1996]. For the profiles described above, the average C$_2$H$_2$/CO ratio was 2.75 at 1.1 km, which suggested that the plume was less than 5 days old.

[21] The ozone-enhanced layers between 0.9 and 1.8 km (Figure 2d) may result from photochemistry during transport. The concentrations of ethane and propane were higher in the CBL than the layer above the CBL. This is consistent with the higher CO concentrations in the CBL than just above it. The ethane and propane above the CBL may have contributed to the photochemical production of O$_3$. However, the air masses between CBL top and 5.5 km may have different origins.

[22] The SO$_2$ concentrations in the CBL appeared to be determined largely by entrainment. The sharp change in SO$_2$ concentrations at the CBL top and the low SO$_2$ concentrations in the CBL indicates that if the SO$_2$ was initially transported in the CBL (as CO appeared to be) it was effectively being removed. In the well-mixed CBL, SO$_2$ could be lost to the ocean surface or sea salt aerosols efficiently. The SO$_2$ above the CBL appeared to have been transported from its sources above the CBL and below the
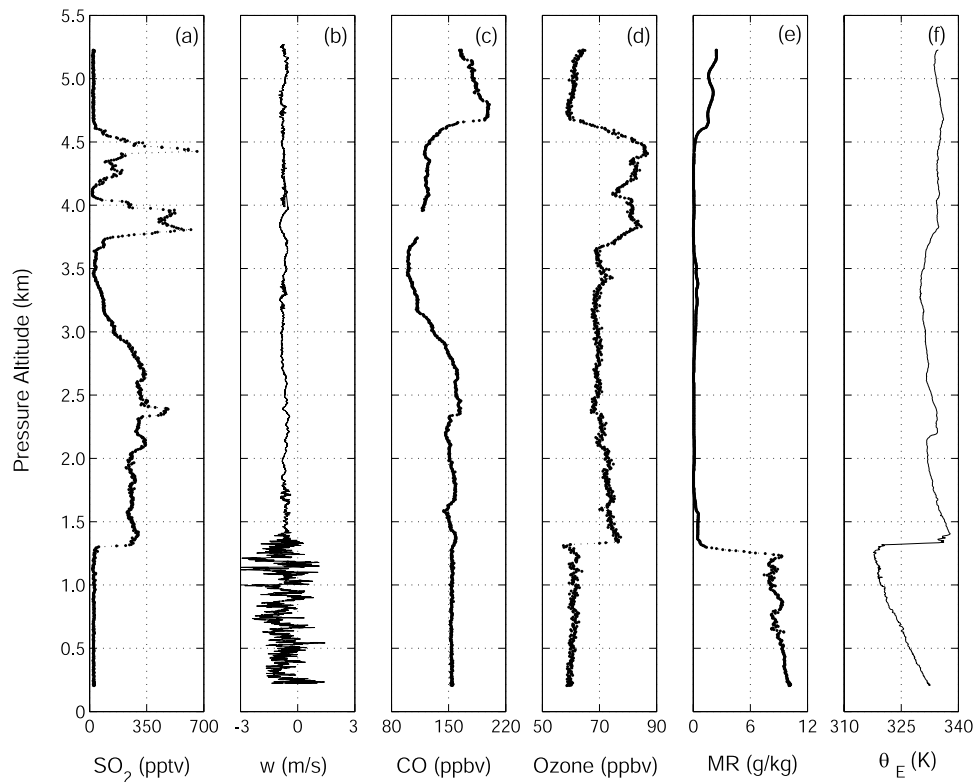
Figure 3. Vertical descent profiles of (a) SO_2, (b) vertical wind velocity (w) indicating turbulence, (c) CO, (d) O_3, (e) water vapor mixing ratio (MR), and (f) equivalent potential temperature (θ_E) near 26.5°N 179°E (southwest of Midway) during flight 21. Data are 1 Hz except for 10 Hz w. The SO_2 layers between 1.3 and 4.6 km were associated with low turbulence in dry air. The CO profile suggested that the SO_2 layers between 1.3 and 3.0 km had more anthropogenic influence than the SO_2 layers between 3.75 and 4.6 km.

extensive dry layer aloft. Assuming an entrainment velocity of 0.5 cm/s and a deposition velocity of 1 cm/s, the CBL SO_2 concentration of 80 pptv is in approximate balance with the 500 pptv SO_2 above the CBL.

[23] The nighttime vertical profiles shown in Figure 3 were obtained at 26.5°N 179.2°E near Midway Island (flight 21). Large changes in w, SO_2, O_3, and water vapor at 1.3 km identified the CBL top. The SO_2-enhanced layers associated with the elevated O_3 and CO concentrations in very dry air were observed above the well-mixed CBL between 1.3 and 4.6 km (Figure 3). The back trajectory (Figure 6, dashed line with diamonds) showed that the air parcels near 2.5 km descended from 9 km 2 days before flight 21. The subsiding air parcels were dry and had low turbulence (less than ±0.1 m/s). The strong inversion (Figure 3f) isolated the subsiding air from the CBL and dry air is less likely to be entrained into the CBL as fast as moist air. The SO_2 in dry air above the CBL could be transported farther from its sources when SO_2 was decoupled from the boundary layer.

[24] The lower free troposphere in Figure 3 can be divided into three sections having substantially different characteristics: 1.3–3.5 km (lower), 3.5–4.6 km (middle), and above 4.6 km (upper). The upper and lower levels had relatively elevated CO, ethane, and propane concentrations compared to the middle layer. The top layer was differentiated from the lower two layers by having higher water vapor and lower ozone. The middle layer had elevated SO_2 and O_3 concentrations with lower CO concentrations than the surrounding layers, which suggested that these layers had different origins and different pathways during transport to the regions near Midway.

[25] Profiles for SO_2, w, CO, O_3, MR and θ_e shown in Figure 4 were obtained at 27.7°N 178.8°W near the end of flight 21. These profiles (Figure 4) had similar features to those near the beginning of the flight (Figure 3). At the end of the flight, there were clouds in the upper layer, which explained the high turbulence in this region and the very low concentrations of SO_2 (<20 pptv). The upper layer was also characterized by enhanced CO and lower O_3 concentrations. The middle and lower levels were characterized by extremely low water vapor. However, the CO was enhanced in the lower level and O_3 was enhanced in the middle level. SO_2 is present in both the middle and the lower levels with a distinct peak (1.3 ppbv) at the top of the middle level.

[26] The C_2H_2/CO ratios were 1.27 at 5 km, 2.1 at 4.5 km and 2.25 at 3 km. This is consistent with the observation that the ethane and propane concentrations at 4.5 km were about double the concentration at 5.5 km and the concentrations at 3 km were almost 2.5 times greater than at 5.5 km. These data indicated that the age of the air mass above 5.5 km was older than the free tropospheric air masses below.

[27] On flight 22, the back trajectories (Figure 6, dotted line with circles) showed that the air masses at 24.8°N
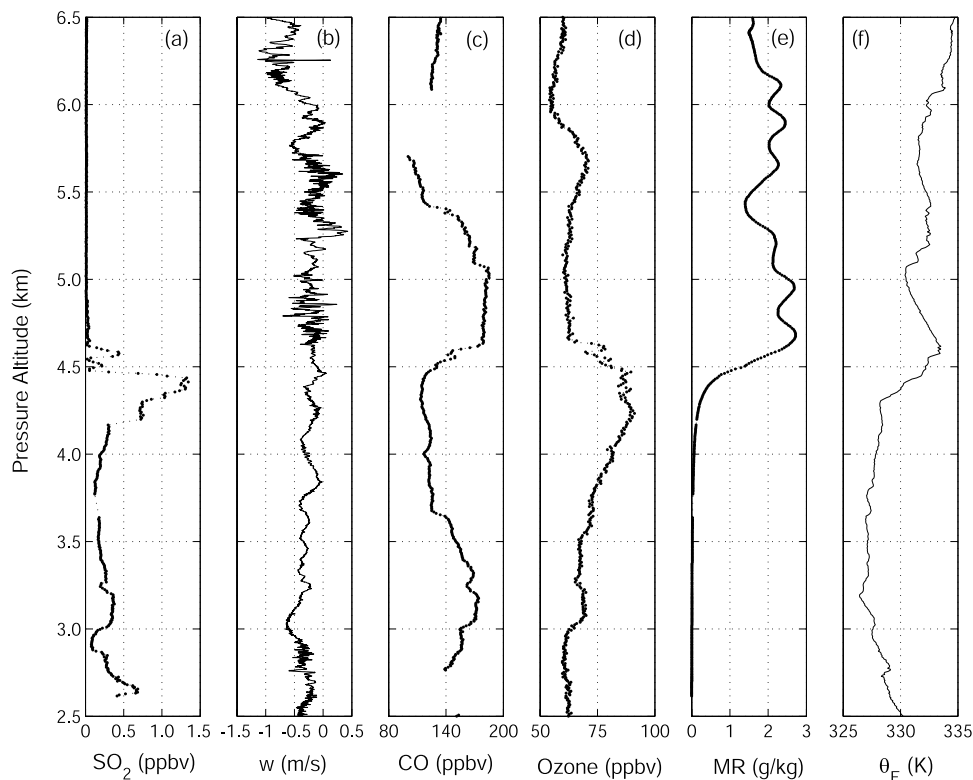
Figure 4. Vertical descent profiles of (a) SO$_2$, (b) vertical wind velocity (w) indicating turbulence, (c) CO, (d) O$_3$, (e) water vapor mixing ratio (MR), and (f) equivalent potential temperature (θ_E) near 27.7°N 178.8°W (west of Midway) during flight 21. Data are 1 Hz except for 10 Hz w. The increase in water vapor near 4.5 km indicated two different air masses. The air above 4.6 km was associated with enhanced CO and intermittent turbulence possibly from a dissipated cloud. The SO$_2$ layers below 4.6 km were associated with enhanced O$_3$, low turbulence, and low water vapor.

177.5°W came from the same area where the profiles (Figure 3) were obtained during flight 21. Although, the flight 22 flight plan was limited in altitude range compared to flight 21 (Figure 3), similar features were observed in the flight 22 profiles (Figure 5). The SO$_2$-enhanced layers were associated with low water vapor and low turbulence between 2.2 and 3.7 km (Figures 5b and 5e). The shear-produced turbulence (Figure 5b) and inversion (Figure 5f) at 3.17 km indicates a separation of two different air masses. The SO$_2$ layers below 3.17 km were associated with enhanced CO and the SO$_2$ layers above 3.17 km were associated with enhanced ozone. The average C$_2$H$_2$/CO ratio was 2.3 below 3 km and 1.7 above 3 km. The average ethane and propane concentrations above 3.17 km were about 50% of the concentrations below 3.17 km. The air mass below 3.17 km appeared to be a remnant of an urban plume.

[28] In general, the air masses at different altitudes had different atmospheric chemical signatures. These air masses might have had different origins and were transported by varying pathways before they arrived in the central Pacific. The low turbulence condition limited the vertical mixing between different air masses. The air masses at similar altitudes had similar atmospheric chemical features indicating that the air masses might have the same origin and follow the same transport route to the central Pacific. However, the chemical concentrations were not horizontally

uniform, which might be due to the source variation and horizontal diffusion.

[29] As described above, the profiles observed near Midway Island were very complex. The 5-day back trajectories shown in Figure 6 could not illustrate the origins and the pathway for the air masses encountered near Midway. To better understand the origins and pathways of these air masses encountered near Midway, a set of 7-day back trajectories were generated for the profiles in flight 21 and 22 using the HYSPLIT model. The nominal altitudes, which were from 0.25 to 6.5 km with 0.25 km spacing, were used as the starting altitudes. The aircraft locations along each profile at the nominal altitudes were used as the starting location. Illustrative HYSPLIT back trajectories for the SO$_2$ layers encountered on flight 21 and 22 are shown in Figure 7.

[30] For the enhanced-CO (Figures 2c, 3c and 4c) and hydrocarbon layers above 4.5 km, the trajectory (solid lines with diamonds, Figure 7) indicated that air masses from south Asia were transported to the central Pacific in 7 days through an eastern route. These layers were also associated with wet air conditions and SO$_2$ was always below 50 pptv above 4.5 km. The SO$_2$ appeared to have been removed from these layers during transport by heterogeneous processing. For the air masses between 1.3 and 4.6 km, the air parcels usually subsided from 6 km or higher altitude, which could account for the lower humidity. For air masses between 3.5 and 4.6 km, the trajectories usually came from
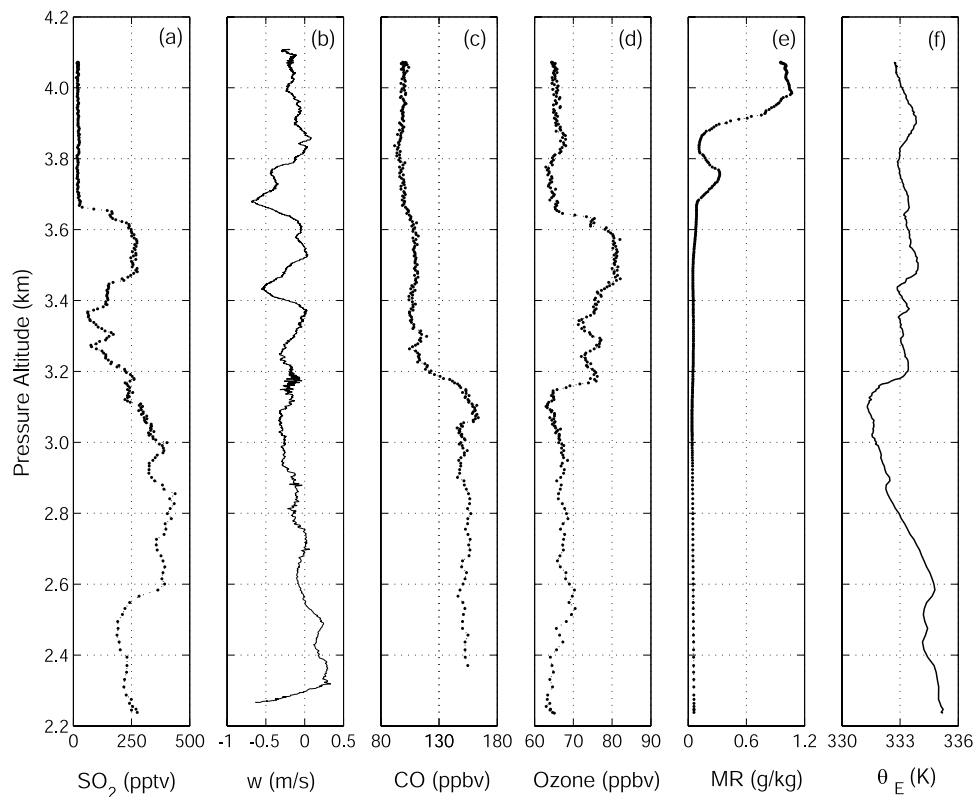
Figure 5. Vertical descent profiles of (a) SO$_2$, (b) vertical wind velocity (w) indicating turbulence, (c) CO, (d) ozone, (e) water vapor mixing ratio (MR), and (f) equivalent potential temperature (θ_e) near 24.8°N 177.5°W (south of Midway) during flight 22. Data are 1 Hz except for 10 Hz w. The profiles had features similar to the profiles for the previous day (Figure 3). The SO$_2$-enhanced layers were associated with low turbulence in dry air. The shear-produced turbulence and inversion at 3.17 km indicated a separation of two different air masses.

west of 120°E above 6 km. The SO$_2$ between 3.5 and 4.6 km could have come from western Asia or Eastern Europe and the age of the plumes would have been older than 7 days. For the air masses between 1.3 and 3.5 km, the trajectory (solid lines with triangles, Figure 7) indicated that the air parcels were moving east below 2 km from Shanghai to Japan and then passed over the Miyake-jima volcano 5 days prior to arriving in the central Pacific. These air parcels were lifted above 6 km and followed the northeastern route arriving in the central Pacific within 4 days. The trajectory indicated the air masses between 1.3 and 3.5 km were mixed with anthropogenic and volcanic emissions and the age of the plumes were not older than 5 days. The trajectories were in agreement with the atmospheric chemical composition discussed above.

3.4. Foundations for Long Range SO$_2$ Transport

[31] The SO$_2$-enhanced layers associated with low turbulence and low water vapor were the most important features in the profiles shown above. *Cho et al.* [2003] characterized the turbulence and stability of the free troposphere from the TAMMS data during the TRACE-P mission. Their work indicated that the transport occurred in layers, which were bounded by thin turbulent layers, and would therefore maintain their integrity over significant distances. For the SO$_2$ transport, *Tu et al.* [2003] reported the observations over the Yellow Sea during the TRACE-P mission flights 13

and 14. These observations indicated that the SO$_2$ transport usually occurred in layers characterized by low turbulence and were often further constrained by temperature inversions. In this work, the observations indicated that the long-range SO$_2$ transport not only occurred in the layers constrained by the atmospheric dynamics but also in low water vapor conditions. The low water vapor concentrations limited the photochemical loss of SO$_2$ by hydroxyl radical and aqueous-phase reactions would have been slowed.

[32] In Figures 2 and 3, the SO$_2$-enhanced parcels subsided from higher altitudes where their downward motion slowed forming the layer just above the CBL. The subsiding air with low turbulence was slowly entrained into the CBL. Furthermore, dry subsiding air does not entrain into the CBL as fast as moist air. The entrainment process thus slowed the transport of SO$_2$ into the CBL from above. Once the SO$_2$ is entrained into the CBL, the SO$_2$ is efficiently lost to aerosols or the ocean surface. Overall, the isolation of SO$_2$ from the ocean surface with dry and low turbulence atmospheric conditions could have been the foundations for the long-range SO$_2$ transport.

3.5. SO$_2$ Transport Connected to the East Asia Outflow

[33] Most of the back trajectories from the central Pacific near Midway (Figures 6 and 7) passed over eastern China, Japan, and Korea. Earlier in the TRACE-P mission, a series of research flights were conducted between eastern China,
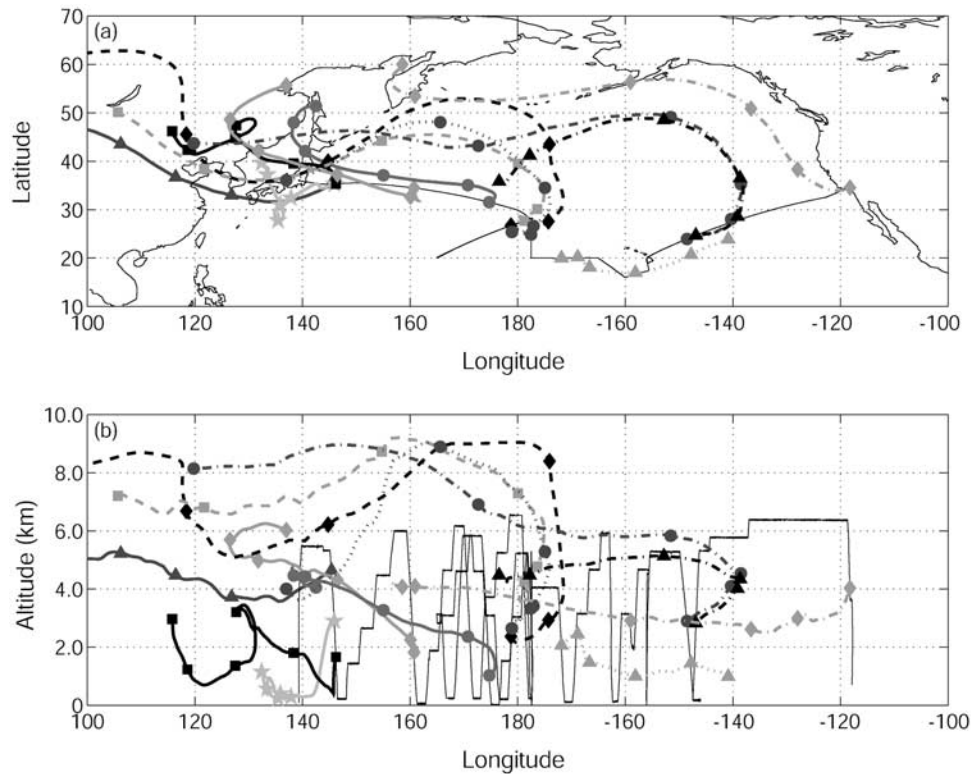
Figure 6. The typical 5-day back trajectories for those enhanced SO₂ layers shown in Figure 1. (a) Horizontal tracks of back trajectories. (b) Altitude profiles of the back trajectories. Flight 20 (heavy solid lines), Flight 21 (dashed lines), Flight 22 (dotted lines) and Flight 23 (dot-dashed lines). Each symbol represents 1-day intervals. The thin solid lines indicate the flight tracks.

Japan, and Korea. Flights 18 and 19 were the only two research flights in the proper time frame associated with the back trajectories for flights 20–22. Flight 18 was flown on 30 Mar 2001, which was 5 days before flight 20, and flight 19 was flown on 2 April 2001, which was 4 days before flight 21 and 5 days before flight 22. The flight plan for flight 18 was to study Asian outflow to the Sea of Japan and flight 19 was to study the warm conveyor belts (WCBs) associated with the cyclonic activity and the interleaving of stratospheric and pollution influences on the back side of the cyclones [*Fuelberg et al.*, 2003; *Jacob et al.*, 2003].

[34] For flight 18 (Figures 8a and 8b), the SO₂ concentrations above 4 km were usually below 500 ppt, except at the beginning of the flight where the aircraft flew west toward Korea above the Sea of Japan. Over 1 ppbv of SO₂ was encountered at 5.4 km in 37.3°N 135.0°E. The average SO₂ concentration above 4 km was 195 pptv and the average SO₂ concentration from the surface to 4 km was 765 pptv. SO₂ plumes were observed below 4 km over the east Yellow Sea and southwestern Japan during flight 18. The maximum SO₂ concentration between 2 and 4 km was 7.5 ppbv and the average SO₂ concentration was 362 pptv. The maximum SO₂ concentration during the flight was 9.5 ppbv at 0.45 km in 29.1°N 130.1°E and the average SO₂ concentration below 2 km was 1.0 ppbv.

[35] On flight 19 (Figures 8c and 8d), plumes of SO₂ >1 ppbv were mainly encountered below 2 km before 0600 UTC. A plume with 5–12 ppbv of SO₂ was encountered between 2.5 and 4 km around 0620–0710 UTC. The average SO₂ concentration below 2 km was 1.3 ppbv and the average SO₂ concentration between 2 and 4 km was 3.5 ppbv. For altitudes above 4 km, the SO₂ concentrations were mainly below 500 pptv, however, a plume with 3.4 ppbv of SO₂ was encountered from 4.0 to 4.4 km near 40.7°N 136.5°E. For both flights, the high SO₂ concentration was mainly observed below 4 km.

[36] Forward trajectories were used to study the movements of air parcels for flights 18 and 19 to better understand the SO₂ transport routes to the central Pacific. Two sets of 5-day forward trajectories were generated for flights 18 (Figures 9a and 9b) and 19 (Figures 9c and 9d) using the HYSPLIT model. Each set included the forward trajectories along the flight tracks at six different altitudes each hour during the SO₂ data recording time. The starting points of the HYSPLIT trajectories were the P-3B aircraft locations on each UTC hour. The nominal starting altitudes were 0.5, 1, 2, 3, 4, and 5 km. The P-3B pressure altitude was used as the starting altitude and replaced one of the nominal HYSPLIT starting altitudes on each UTC hour. There were a total of 42 trajectories for flight 18 and 48 trajectories for flight 19. Only the trajectories starting at the aircraft location are plotted in Figure 9.

[37] In general, for flight 18, the forward trajectories that started above 4 km usually followed the northeastern route and arrived in the central Pacific between 170°E–160°W and 40°–60°N within 3 days. The forward trajectories between 2 and 4 km usually first descended to low altitude, moved toward the southeast in a circular route, and arrived
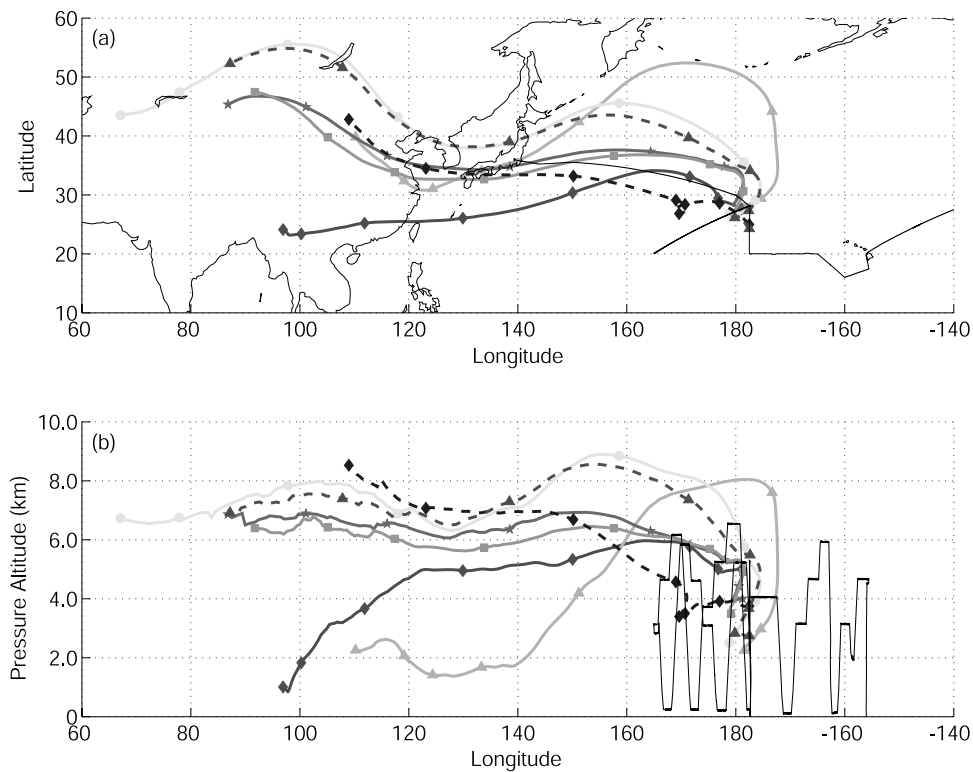
Figure 7. Selected Hybrid Single-Particle Lagrangian Integrated Trajectory (HYSPLIT) model 7-day back trajectories for flight 21 (solid lines) and 22 (dashed lines). (a) Horizontal tracks of back trajectories. (b) Altitude profiles of the back trajectories. Each symbol represents a 1-day interval. The air masses above 4.5 km (solid lines with diamonds) came from south Asia and were older than 7 days. The air masses between 1.3 and 3.5 km (solid lines with triangles) were influenced by both anthropogenic and volcanic emissions.

in a region south of 35°N and west of 160°E within 2–3 days. The air parcels, in the region south of 35°N and west of 160°E, tended to stay low and followed the eastern route moving to the central Pacific, or the air parcels were lifted up above 4 km and followed the northeast route arriving in the central Pacific in another 2 days. The forward trajectories that started below 2 km usually circled below 2 km in an area adjacent to the starting point. The forward trajectories for flight 18 suggested that the air parcels above 4 km were transported into the central Pacific efficiently; however, the major SO₂ outflow from east Asia was usually transported below 4 km. Less SO₂ was transported above 4 km and had less impact to the central Pacific environment. The highest SO₂ concentrations were usually encountered below 2 km. The forward trajectories suggested that the air parcels below 2 km usually stayed at low altitudes over the southeastern Japan and Yellow Sea area and had less chance to be transported to the central Pacific. Overall, on the basis of the trajectories and SO₂ concentrations, the SO₂ transported between 2 and 4 km would dominate the SO₂ concentration in the central Pacific.

[38] On flight 19, the forward trajectories above 3 km showed that the air parcels first followed the northeastern route moving east between 40° and 60°N and reached 170°W within 2 days. The air parcels in the central Pacific followed another circular route moving farther east and arrived at 150°W in another 3 days. The trajectories below

3 km showed that the air parcels first followed the northeastern route toward the Kamchatka Peninsula while they ascended to a higher altitude. The air parcels near Kamchatka Peninsula mainly followed the air parcels above 3 km and moved east toward the central Pacific. Some of the air parcels circled above the Kamchatka Peninsula and then descended toward the Bering Sea and Alaska. On flight 19, the forward trajectories, arriving in the central Pacific (Figures 9c and 9d), were similar to the back trajectories for flight 21 and 22 (Figures 6 and 7). The similarities of the trajectories indicated that the SO₂-enhanced layers in the central Pacific had strong connections with the Asian outflow.

[39] In earlier model studies, *Xiao et al.* [1997] showed that the major Asian outflow occurred in the latitude band of 30° to 40°N and below 4 km. The Asian outflow was associated with the cold fronts, which passed through east Asia. *Bey et al.* [2001] showed that the eastward moving cold fronts are the principal process responsible for export of chemical outflow from Asia. Their studies concluded that the major Asian outflow to the Pacific were associated with frontal movement and transport in the lower troposphere (2–5 km). A front passed the study area of flight 19 on 1 April 2001, which was 1 day before flight 19. The layer of plumes observed between 2.5 and 4 km on flight 19 were associated with frontal movement and could have had more influence on the central Pacific than the SO₂ plumes below
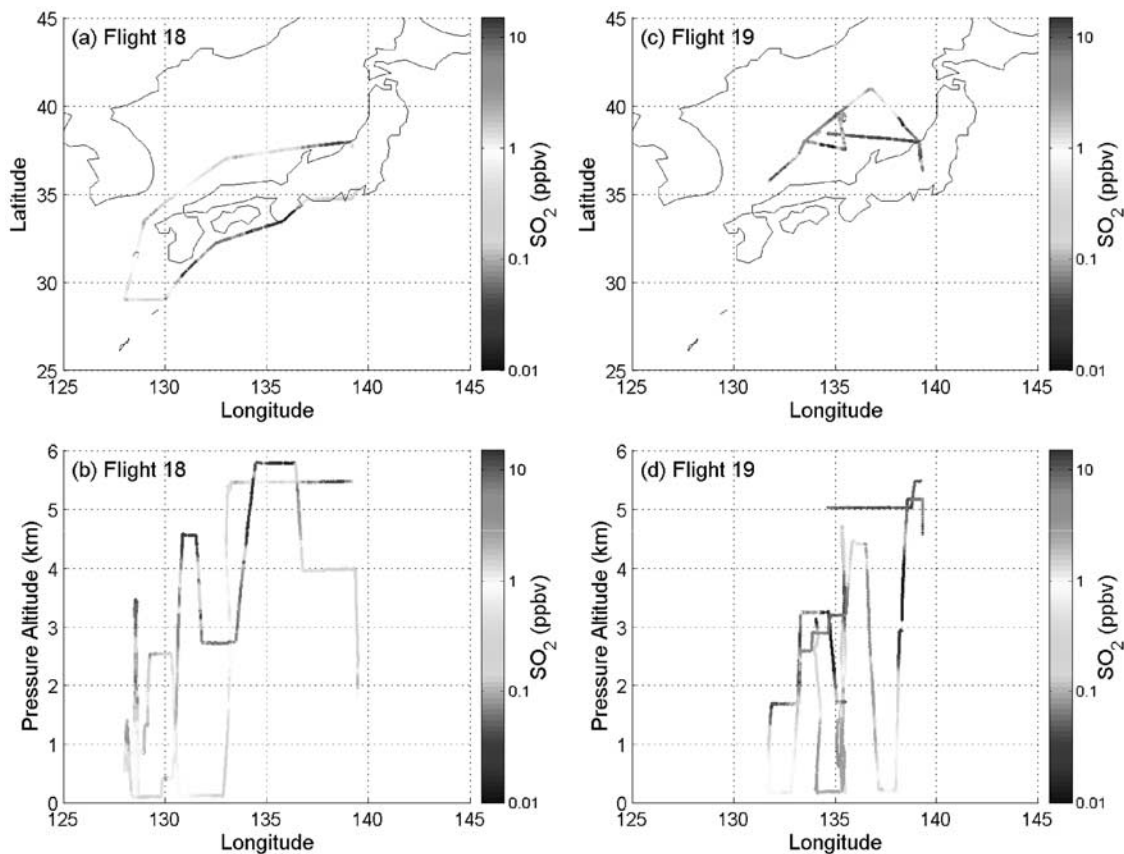
Figure 8. The SO₂ distributions along the tracks for (a, b) flight 18 and (c, d) flight 19. Note the major SO₂ outflow was between 1 and 5 km. See color version of this figure at back of this issue.

2 km. The frontal movement was responsible for lifting the SO₂ to the lower free troposphere where the SO₂ was transported to the central Pacific.

3.6. Volcano Influence

[40] In March and April 2001, the Miyake-jima volcano (34.1°N, 139.5°E, and 813 m) had an average SO₂ flux of 1118 ton/hr (K. Kazahaya, personal communication, 2003). The SO₂ emissions from the Miyake-jima volcano were equal to the total daily average of SO₂ emissions (based on annual average) from the six largest SO₂ source regions in China [*Streets et al.*, 2003]. In Figure 7, the trajectories, which passed by the Miyake-jima volcano, indicated that the volcanic emissions could have had significant contributions to the SO₂ observed in the central Pacific. Using the HYSPLIT model, several 5-day forward trajectories were generated using the Miyake-jima volcano as a starting point. The forward trajectories covered the dates between 28 March 2001 and 5 April 2001. Each set of forward trajectories included six trajectories started between 0.5 and 3 km with 0.5 km increments. The trajectories began at 0000 hour UTC of each day.

[41] Inspection of the forward trajectories beginning at Miyake-jima on 1 April 2001 (Figures 10a and 10b) revealed that air parcels, which started at Miyake-jima, moved eastward for one day, moved north on the second day, and then passed the flight 20 flight path. A comparable back trajectory is shown in Figure 6 (solid line with stars). The SO₂-enhanced layer at 2.5 km early in flight 20

(Figure 1) was influenced by the Miyake-jima volcano. The forward trajectories on 3 April 2001 (Figures 10c and 10d) showed that the air parcels were lifted above 3 km and transported to the central Pacific near Midway Island within 3 days following the northeastern route. Both flight 21 (6 April 2001) and flight 22 (7 April 2001) were likely influenced by the Miyake-jima volcano.

3.7. Model Comparisons

[42] In this paper, we presented SO₂ observations in the central Pacific. Trajectory tools were used to help identify the sources and transport routes. However, the observations and the trajectories provided only limited information about how the chemical species were transported and evolved over time. Chemical transport models (CTMs) have proven to be complementary tools in the analyses of large-scale atmospheric chemistry field studies. In the following sections, two CTMs were used to study the SO₂ transport to the central Pacific. By comparing the SO₂ observations with CTM results, we had evaluated the influence from the anthropogenic and volcanic emissions in east Asia to the central Pacific.

[43] The high-resolution chemical modeling system, CFORS/STEM-2K1 [*Carmichael et al.*, 2003], was used to study the transport and chemical evolution of SO₂ as it moves from its sources in Asia to the North Pacific troposphere. The important new features in STEM-2K1 include: (1) the use of the SAPRC99 chemical mechanism [*Carter*, 2000], which consists of 93 species and 225 reac-
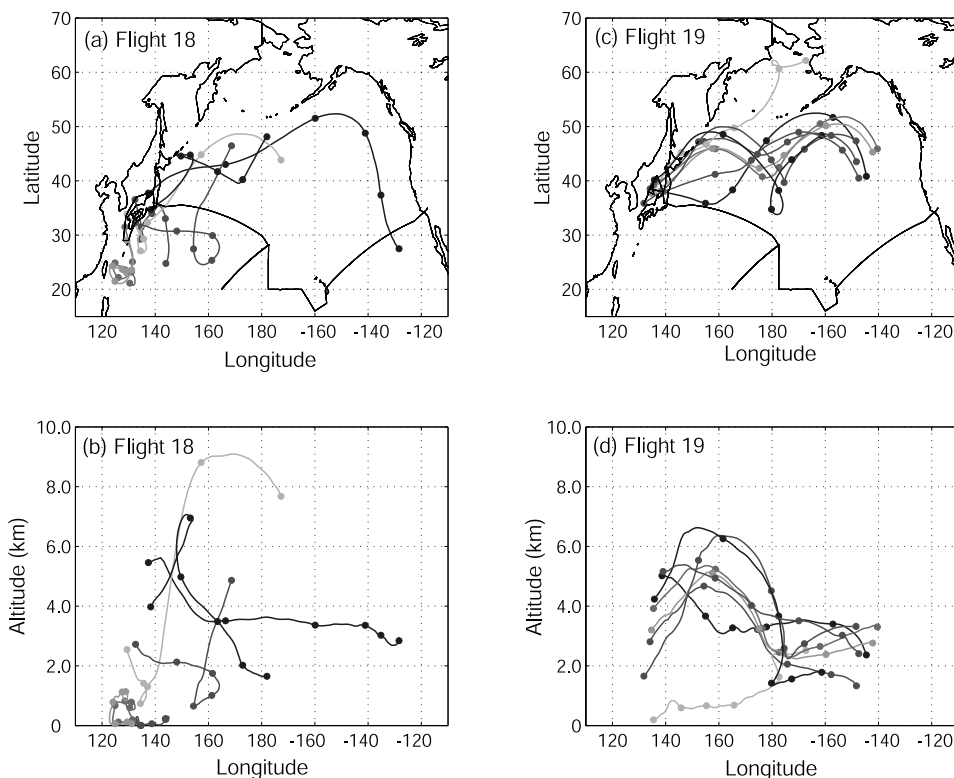
Figure 9. The HYSPLIT 5-day forward trajectories along the tracks for (a, b) flight 18 and (c, d) flight 19. On flight 18, the air parcels below 2 km usually stayed near the starting locations. The air parcels above 2 km were generally efficiently transported to the central Pacific. On flight 19, the trajectories were similar to those shown on Figure 7. The trajectory similarities indicate that the SO₂-enhanced layers in the central Pacific had strong connections with Asian outflow.
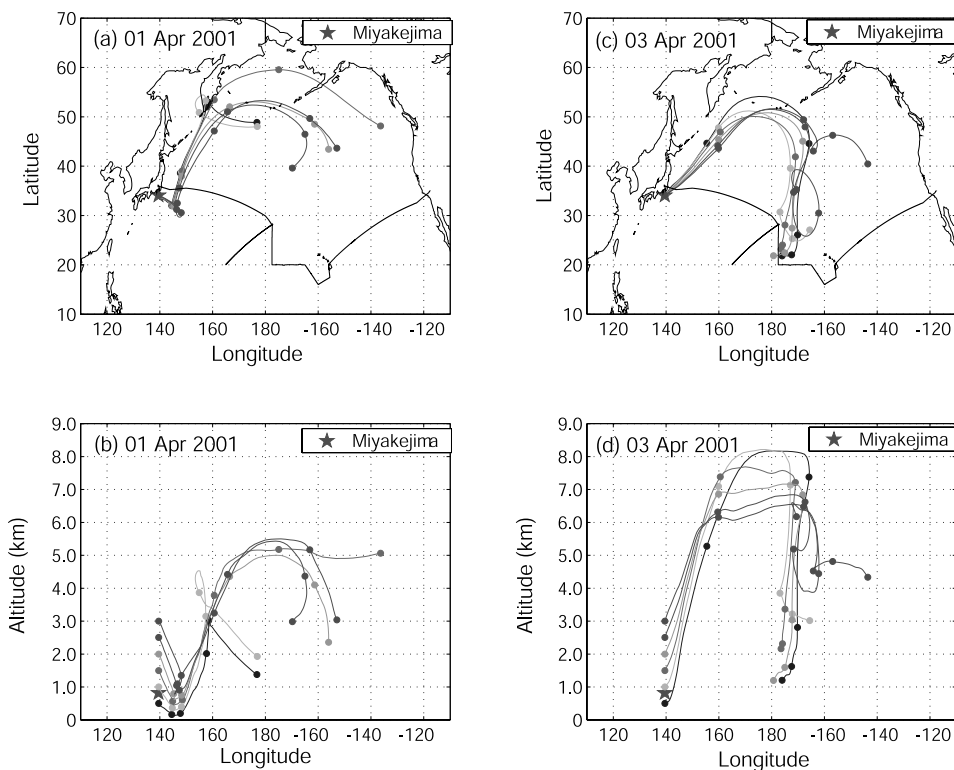

Figure 10. The HYSPLIT 5-day forward trajectories generated for the Miyake-jima volcano on (a, b) 1 April 2001 and (c, d) 3 April 2001. The trajectories indicate that the SO₂-enhanced layers observed during flights 20, 21, and 22 were heavily influenced by the emissions of the Miyake-jima volcano.

tions; (2) the integration of the chemical mechanism using an implicit second-order Rosenbrock method [*Sandu et al.*, 1997]; (3) the calculation of photolysis rates and the influences of cloud, aerosol and gas-phase absorptions due to O_3, SO_2 and NO_2, using the NCAR Tropospheric Ultraviolet-Visible (TUV) radiation model [*Madronich and Flocke*, 1999]; and (4) the extension of the aerosol calculations to include optical information (e.g., extinction) in addition to mass, size and composition. Complete details regarding this model were reported by *Carmichael et al.* [2003] and *Uno et al.* [2003]. However, for TRACE-P, the STEM-2K1 model domain extended only to 155°E, so we could not use it to compare to the SO_2 observations in the central Pacific.

[44] The HYSPLIT model was used to simulate SO_2 dispersion and deposition from both anthropogenic and volcanic emissions from east Asia from which the SO_2 distributions in the North Pacific were predicted. The model was configured as the horizontal top hat puff and the vertical particle model. The model grid was centered at 40°N 180°E and a span of 90° by 180°. The model domain top was 10 km with 19 layers, which were spaced by the relation

$$z = 30k^2 - 25k + 5 \qquad (1)$$

where z is the model's internal height, k is the model's internal index [*Draxler and Hess*, 1997]. The output grid levels were defined as 10 levels from 0.5 to 5 km with 0.5 km spacing. The calculated dispersion results were saved with a horizontal resolution of 0.25 by 0.25 degrees for comparison with the SO_2 observations. At the true air speeds of the P-3B, the resolution of the dispersion results was comparable to 5-min intervals along the flight tracks. The model took into account only atmospheric dynamics with wet and dry deposition of SO_2. The model did not contain any chemical formation or destruction reactions.

[45] The inputs to the model were limited to the six largest SO_2 source regions in China, and the Miyake-jima volcano. The reason for choosing only seven input locations was that the total emission rate from the six largest SO_2 sources was comparable to the emission rate from Miyake-jima volcano. For the China sources, the annual SO_2 emission rates [*Streets et al.*, 2003] were used to estimate hourly emission rates for the model input. For the Miyake-jima volcano, the hourly emission rates were estimated from daily emission rates determined from COSPEC measurements (K. Kazahaya, personal communication, 2003, see also http://staff.aist.go.jp/kazahaya-k/miyakegas/COSPEC.html), during the time of the TRACE-P missions. The model output was the SO_2 concentrations calculated for each level in 1-hour steps. The details of the simulation inputs are listed in Table 1.

[46] Two types of simulations were performed to estimate the influence from the Miyake-jima volcano. The first simulation type included the Miyake-jima volcano and the six largest anthropogenic source regions in China. The second simulation included only the six largest anthropogenic source regions in China. The goal of using the HYSPILT model was to estimate the impact of the volcano in the absence of a true CTM model results.

Table 1. SO_2 Emission Rates and the Starting Locations for Simulations Using the HYSPLIT Model Initiated at 0000 UTC 27 March 2001 for 15 Days

Name	Latitude, deg	Longitude, deg	Altitude, m	Emission Rate, t/h
Miyake-jima	34.1	139.5	813	1118
Shandong	36.6	117.0	100	225
Sichuan	29.5	106.5	500	196
Shanxi	37.8	112.5	500	169
Hebei	39.9	116.4	100	154
Henan	34.7	113.6	100	138
Jiangsu	31.2	121.4	100	136

[47] The STEM-2K1 and HYSPLIT model domains both covered the area for TRACE-P flights 18, 19 and a part of 20. The SO_2 observations, the STEM-2K1 model, and the HYSPLIT model results were compared for these flights. For flight 18 (Figure 11), the STEM-2K1 model results were in good agreement with the SO_2 observations after 0200 UTC. The STEM-2K1 model results had the same trend as the SO_2 observations and the STEM-2K1 model precisely predicted the trend and 240 ppbv of CO concentrations (not shown) between 0040 and 0200 UTC.

[48] The STEM-2K1 model results, however, exceeded the SO_2 observations by factors of 2 to 8. The precise CO predictions of the STEM-2K1 model indicate that the difference between the SO_2 observations and model SO_2 results was not due to the atmospheric transport processes. Further study revealed that rain showers were encountered between 0040 and 0200 UTC and no rain showers along the flight track after 0200 UTC. *Tu et al.* [2003] suggested that the STEM-2K1 model usually overestimated the SO_2 concentrations when precipitation was encountered. The observations during flight 18 suggested that a large fraction of SO_2 had been removed by heterogeneous processing prior to 0040–0200 UTC.

[49] The HYSPLIT model simulation results with (Figure 11b, dots) and without (Figure 11b, crosses) the Miyake-jima volcano inputs were nearly the same throughout flight 18 indicating that the Miyake-jima volcano emissions had very little or no influence in this area. The HYSPLIT and STEM-2K1 predictions were in good agreement with the SO_2 observations after 0420 UTC. The HYSPLIT model results also had a trend similar to the STEM-2K1 results and the SO_2 observations before 0420 UTC. However, the HYSPLIT model results were usually lower than both the STEM-2K1 results and the SO_2 observations. The reason for the HYSPLIT results being lower than STEM-2K1 results could be that the HYSPLIT model did not include all of the SO_2 emission sources that the STEM-2K1 did. The HYSPLIT model simulations used only a simplified six source regions in east China and these regions were south of 40°N. The back trajectories along the flight track showed that the air parcels came from north of 40°N around the northeastern China and the Korean peninsula between 0000 and 0420 UTC. On the other hand, the back trajectories after 0420 UTC came directly from south of 40°N in east China, whose sources were included in both models.

[50] The SO_2 observations, the STEM-2K1 results, and the HYSPLIT results for TRACE-P flight 19 are compared in Figure 12. During flight 19, only small rain showers were encountered and these rain showers occurred only at the end
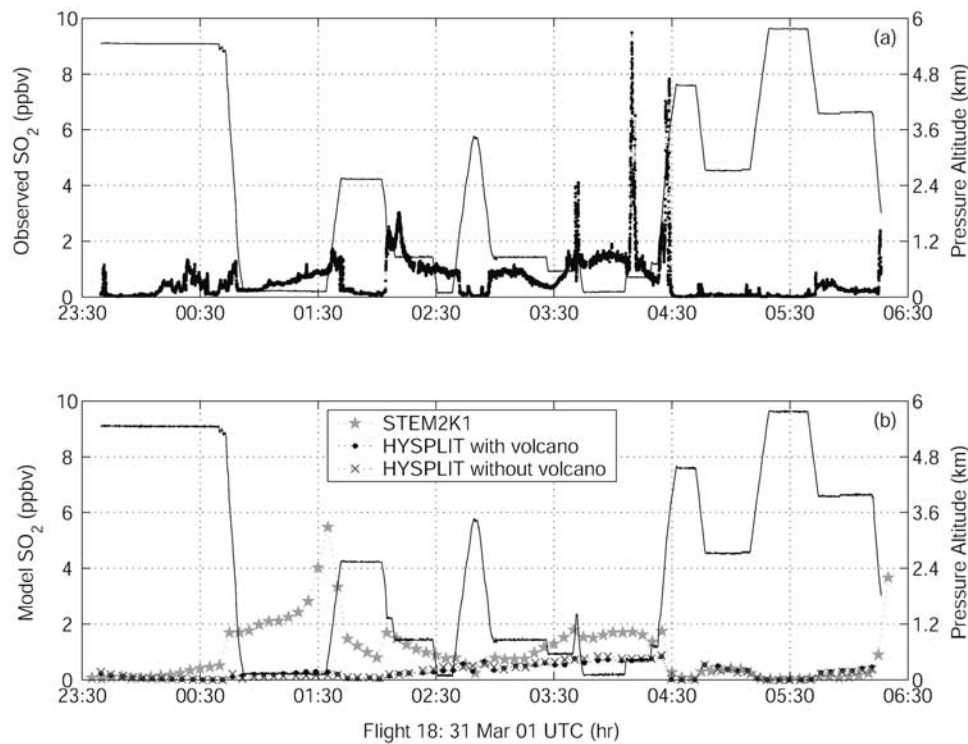
Figure 11. (a) Observed SO$_2$ data and (b) model SO$_2$ results along the flight track for TRACE-P mission flight 18. The STEM-2K1 model overestimated the SO$_2$ concentration before 0200 UTC but had the same trend as the SO$_2$ observations. The HYSPLIT model was used with limited anthropogenic SO$_2$ source inputs. The HYSPLIT results without the volcanic input illustrated that the volcano had very little effect for this flight.
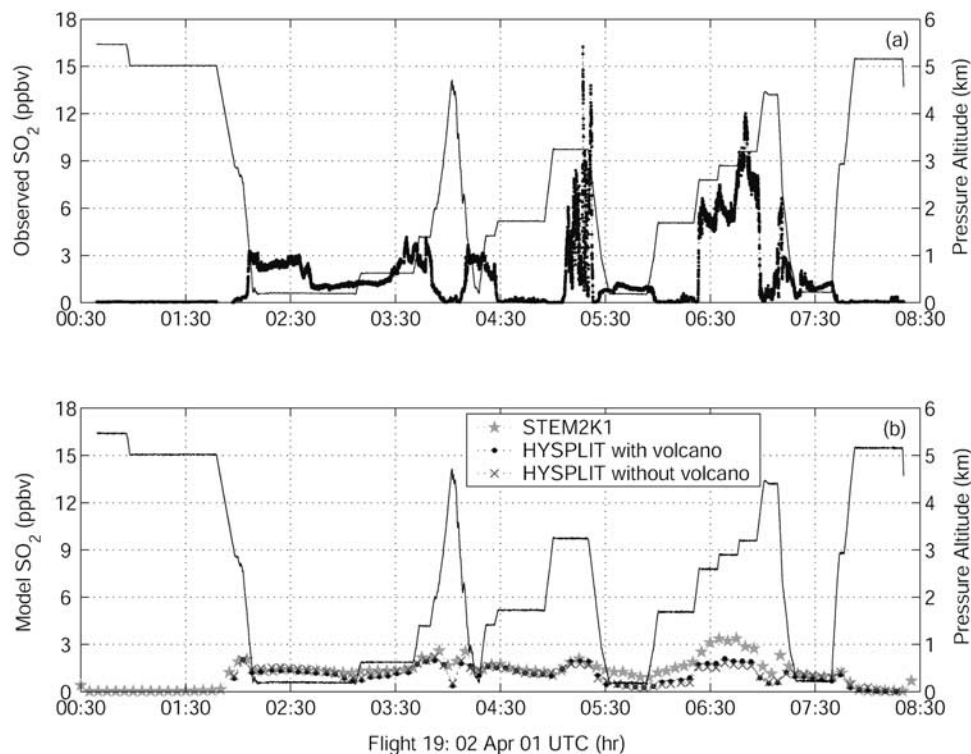

Figure 12. (a) Observed SO$_2$ data and (b) model SO$_2$ results along the flight track for TRACE-P mission flight 19. The results of the two models are in fairly good agreement. The models underestimated the observations in the SO$_2$-enhanced layers. The models overestimated the observations when the SO$_2$ was <200 pptv except after 0730 UTC.
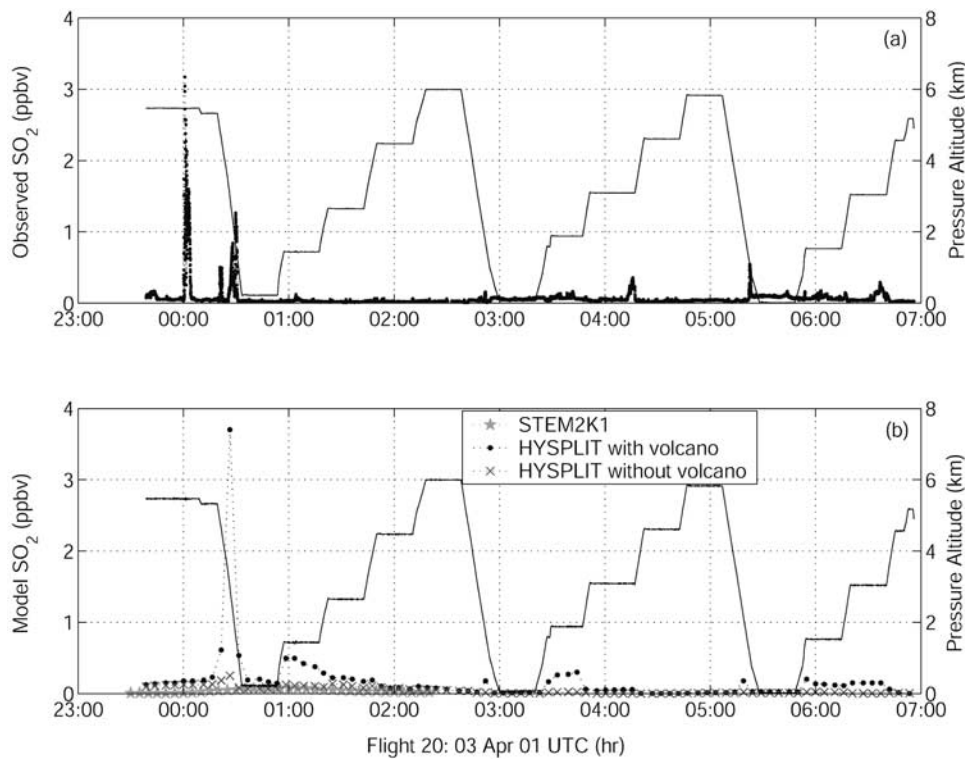
Figure 13. (a) Observed SO$_2$ data and (b) model SO$_2$ results along the flight track for TRACE-P mission flight 20. The STEM-2K1 model domain ended at 155°E. The HYSPLIT model results indicated that the Miyake-jima volcano had a significant influence around 0030 UTC, which is reflected in the observations.

of flight 19 after 0700 UTC. For this case the STEM-2K1 and HYSPLIT agreed with each other and generally followed the same trend as the SO$_2$ observations indicating that both models simulated the SO$_2$ distributions in the atmosphere when the SO$_2$ distributions were controlled only by the atmospheric dynamics, i.e., no effects of heterogeneous processes.

[51] The SO$_2$ observations, the STEM-2K1 results, and the HYSPLIT results for flight 20 are compared in Figure 13. Only the first 1/3 of the flight was in the STEM-2K1 domain. Recall that the trajectories described above (Figures 10a and 10b), suggested that the Miyake-jima volcano had significant influence on flight 20 in creating the SO$_2$-enhanced layer at 2.5 km shown on Figure 1. However, the STEM-2K1 model results did not indicate this result. The STEM-2K1 predicted SO$_2$ concentrations <100 pptv. On the other hand, the HYSPLIT model clearly predicted the impact of the volcano. When the volcano emissions were included, the modeled SO$_2$ results were 8.5 times higher at 0026 UTC than when the volcano emission was not included. The results of the HYSPLIT model simulations with the volcano source exceeded the average SO$_2$ measurements by factors of 2−19 between 0015 and 0200 UTC. This prediction is reasonable because heavy rain showers were encountered during this period and this model does not contain chemistry related to heterogeneous loss in cloud and rain. The precipitation analysis daily images for 3−4 April 2001 from the Tropical Rainfall Measurement Mission (TRMM) microwave imager (TMI) (Global Precipitation Climatology Project, Laboratory

for Atmospheres, NASA Goddard Space Flight Center, http://precip.gsfc.nasa.gov/rain_pages/daily_choice.html) indicated a wide area of 2−5+ cm/day of rain from 30°−40°N and 140°−160°E. The Special Sensor Microwave Imager (SSM/I) on the Defense Meteorological Satellite program (DMSP) for 4 April 2001 showed the 2−8+ cm/day of rain in the same wide area and the heaviest rain (16+ cm/day) was centered on 165°E 40°N. The rainfall analysis suggests that a significant amount of SO$_2$ could have been removed by the heavy rainfall during this period.

[52] The forward trajectories (Figures 10c and 10d) also suggest flights 21 and 22 were influenced by the Miyake-jima volcano in the region of 25°−35°N and 170°E−170°W. The four profiles with enhanced SO$_2$ layers on flights 21 and 22 were compared to the HYSPLIT model results (Figure 14, dots, triangles and circles). The aircraft locations at the profile median time were used to select the HYSPLIT model results. The HYSPLIT model results are very similar to the SO$_2$ profile at the selected locations. The HYSPLIT model predictions between 1 and 4 km for these four profiles without volcano inputs were about 9−30% of the predictions with volcano inputs. This indicates that the observed SO$_2$-enhanced layers were mainly due to the Miyake-jima volcano.

[53] One reason that the volcanic emissions may have had more influence than the anthropogenic emissions in the central Pacific could be the weather patterns near the coastline and the location of the source regions. The major SO$_2$ removal during transport was due to heterogeneous processing. The SO$_2$ emitted from the sources in central or
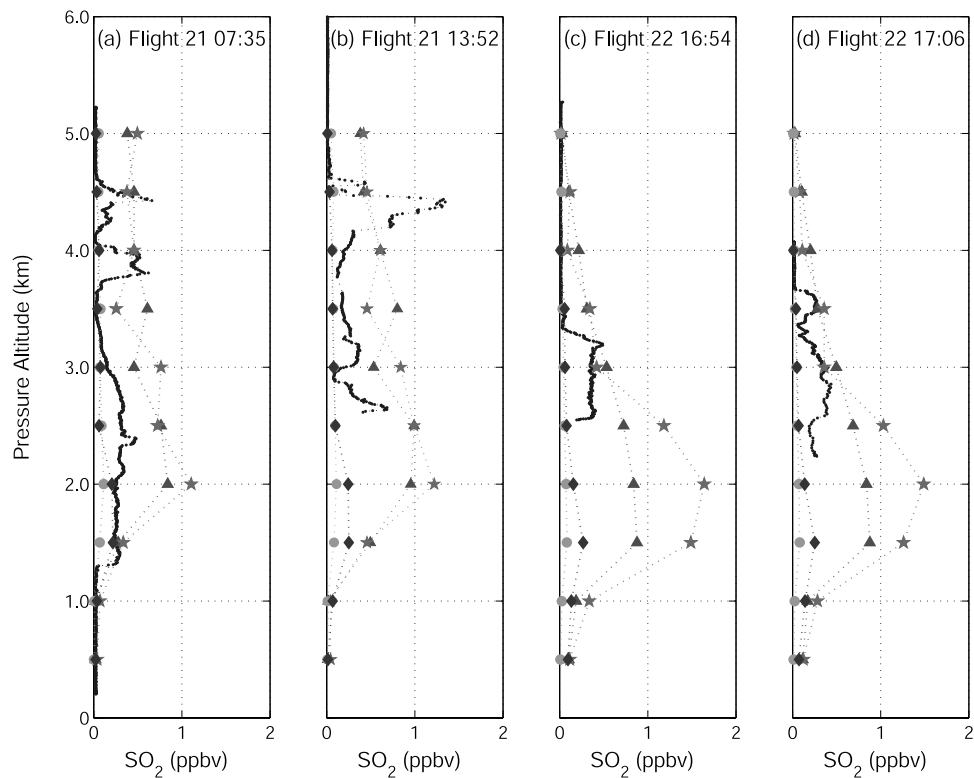
Figure 14. HYSPLIT results for the region of 25°−35°N and 170°E−170°W during flights (a, b) 21 and (c, d) flight 22 illustrating that the Miyake-jima volcano could have had a greater effect than large anthropogenic SO$_2$ sources even if those sources were concentrated in a single location on the Asian continent. Dots are SO$_2$ observations; triangles are model inputs using six anthropogenic source regions and the Miyake-jima volcano; circles are model inputs using six anthropogenic source regions only; stars are model inputs using a combined anthropogenic point source and the Miyake-jima volcano; diamonds are model inputs using combined anthropogenic point source only.

east Asia had more chance to be removed by the rainfall associated with frontal movement. The SO$_2$ emitted from the volcano also starts out at a higher altitude, which may be the primary reason volcanic SO$_2$ appears to have greater chance to be transported to the central Pacific.

[54] Another reason could be that the volcano is a tightly concentrated source. The anthropogenic SO$_2$ source regions are spread over a wide area in central and east Asia. Although, the total amount of SO$_2$ emissions were the same for the volcanic and the six largest regional anthropogenic SO$_2$ sources, the SO$_2$ emissions from anthropogenic sources were more dispersed than those emitted from the volcanic source. Investigating this assumption, two more simulations were performed. In these simulations, the six largest regional anthropogenic source inputs were treated as a point source like the volcano. The model input emissions rate (1018 t/h) for the anthropogenic SO$_2$ emissions was the sum of the six regional anthropogenic SO$_2$ emissions rate used as inputs in previous simulations. The average location (34.95°N 114.6°E, in Henan, China) of the six source regions was used as the starting point. The first simulation included both the combined anthropogenic SO$_2$ point source and the volcanic source (Figure 14, stars). The second simulation was performed using only the combined point source of anthropogenic SO$_2$ (Figure 14, diamonds). In the case of the simulations with volcanic inputs the average model results, between 1 and 3 km, with the

combined anthropogenic point source input were about 1.2−2.4 times higher than the model results with the dispersed six regional source inputs. In the case of the simulations without the volcano input, the average model results with the combined anthropogenic point source input were about 1.1−5.9 times higher than the model results, between 1 and 3 km, with the dispersed six regional source inputs.

[55] When the anthropogenic source regions were treated as one point source, their influences in the central Pacific were increased (Figure 14). The results of this study indicated that a tightly concentrated SO$_2$ plume could be transported farther away. Although, the Miyake-jima volcano was the major SO$_2$ contributor in the central Pacific during March and April 2001, the anthropogenic SO$_2$ emitted from east Asia was dispersed over a wider area and would have impacted a larger area than a volcano. However, it is clear during that time that the volcanic SO$_2$ dominated the SO$_2$ distributions in the central Pacific.

4. Conclusions

[56] In this work, we presented the observations made in the central North Pacific during the NASA TRACE-P mission. Together with trajectory tools and a CTM, the origins and the routes of the SO$_2$ transport were identified. The SO$_2$ emitted from east Asian sources was generally

transported to the central Pacific in 3−4 days. The SO$_2$ distributions during the long-range transport were determined primarily by the atmospheric dynamics.

[57] The SO$_2$-enhanced layers were usually associated with low water vapor and low turbulence. The low water content limited both gas and liquid phase SO$_2$ oxidization. The SO$_2$-enhanced layers with low turbulence maintained their integrity over great distances. The major SO$_2$ removal appeared to be heterogeneous processing (loss to cloud droplets, rainout, washout) in the free troposphere and loss to sea salt aerosols or the ocean surface in the CBL.

[58] The SO$_2$-enhanced layers in the central Pacific usually subsided from a higher altitude and lay on the top of CBL. These layers were usually dry and stable. The slow entrainment process limited the SO$_2$ mixing into the CBL. Consequently, the SO$_2$ layers were effectively isolated from the ocean surface. These factors provided the foundations for long-range SO$_2$ transport.

[59] Trajectories studies showed that the major SO$_2$ transport routes occurred in the midlatitudes (30°−60°N) and the lower troposphere (2−4 km). Both anthropogenic and volcanic sources in east Asia had direct influence on SO$_2$-enhanced layers in the central Pacific. The model simulations indicated that the Miyake-jima volcano was a major contributor of SO$_2$ in the central Pacific. The intense volcanic SO$_2$ source was in a small area and the tightly concentrated SO$_2$ plume appeared to be transported in a coherent way farther than the plumes from the widespread anthropogenic sources. The volcanic SO$_2$ emissions also may have had less chance of removal by precipitation because of the weather patterns at the location of the volcano. The anthropogenic SO$_2$ emissions in east Asia were removed by precipitation when the eastward moving front had rainfall in the east Asia and offshore. The highest SO$_2$ concentrations from east Asia usually were observed in the air masses behind the fronts.

[60] The volcanic SO$_2$ emissions from the Miyake-jima volcano dominated the SO$_2$ distribution in the central Pacific during the spring 2001. The anthropogenic SO$_2$ sources were spread over a wide area so that their influences were diminished in the central Pacific compared to their impact over the Pacific near east Asia.

References

Andreae, M. O., H. Berresheim, T. W. Andreae, M. A. Kritz, T. S. Bates, and J. T. Merrill (1988), Vertical distribution of dimethylsulfide, sulfur dioxide, aerosol ions, and radon over the northeast Pacific Ocean, *J. Atmos. Chem.*, *6*(1−2), 149−173.

Bailey, R., L. A. Barrie, C. J. Halsall, P. Fellin, and D. C. G. Muir (2000), Atmospheric organochlorine pesticides in the western Canadian Arctic: Evidence of transpacific transport, *J. Geophys. Res.*, *105*(D9), 11,805−11,811.

Bandy, A. R., D. C. Thornton, and A. R. Driedger (1993), Airborne measurements of sulfur dioxide, dimethyl sulfide, carbon disulfide, and carbonyl sulfide by isotope dilution gas chromatography mass spectrometry, *J. Geophys. Res.*, *98*(D12), 23,423−23,433.

Bey, I., D. J. Jacob, J. A. Logan, and R. M. Yantosca (2001), Asian chemical outflow to the Pacific in spring: Origins, pathways, and budgets, *J. Geophys. Res.*, *106*(D19), 23,097−23,113.

Carmichael, G. R., et al. (2003), Regional-scale chemical transport modeling in support of the analysis of observations obtained during the TRACE-P experiment, *J. Geophys. Res.*, *108*(D21), 8823, doi:10.1029/ 2002JD003117.

Carter, W. (2000), Documentation of the SAPRC-99 chemical mechanism for voc reactivity assessment, final report to California Air Resources Board, contract no. 92-329, Univ. of Calif., Riverside.

Cho, J. Y. N., R. E. Newell, B. E. Anderson, J. D. W. Barrick, and K. L. Thornhill (2003), Characterizations of tropospheric turbulence and stability layers from aircraft observations, *J. Geophys. Res.*, *108*(D20), 8784, doi:10.1029/2002JD002820.

Clarke, A. D., W. G. Collins, P. J. Rasch, V. N. Kapustin, K. Moore, S. Howell, and H. E. Fuelberg (2001), Dust and pollution transport on global scales: Aerosol measurements and model predictions, *J. Geophys. Res.*, *106*(D23), 32,555−32,569.

Draxler, R., and G. D. Hess (1997), Description of the HYSPLIT-4 modeling system, *NOAA Tech. Memo., ERL ARL-224*.

Draxler, R., and G. D. Hess (1998), An overview of the HYSPLIT-4 modeling system for trajectories, dispersion, and deposition, *Aust. Meteorol. Mag.*, *47*, 295−308.

Duce, R. A., C. K. Unni, B. J. Ray, J. M. Prospero, and J. T. Merrill (1980), Long-range atmospheric transport of soil dust from Asia to the tropical North Pacific: Temporal variability, *Science*, *209*(4464), 1522−1524.

Fuelberg, H. E., R. O. Loring Jr., M. V. Watson, M. C. Sinha, K. E. Pickering, A. M. Thompson, G. W. Sachse, D. R. Blake, and M. R. Schoeberl (1996), TRACE A trajectory intercomparison: 2. Isentropic and kinematic methods, *J. Geophys. Res.*, *101*(D19), 23,927−23,939.

Fuelberg, H. E., C. M. Kiley, J. R. Hannan, D. J. Westberg, M. A. Avery, and R. E. Newell (2003), Meteorological conditions and transport pathways during the Transport and Chemical Evolution over the Pacific (TRACE-P) experiment, *J. Geophys. Res.*, *108*(D20), 8782, doi:10.1029/ 2002JD003092.

Harris, J. M., P. P. Tans, E. J. Dlugokencky, K. A. Masarie, P. M. Lang, S. Whittlestone, and L. P. Steele (1992), Variations in atmospheric methane at Mauna Loa observatory related to long-range transport, *J. Geophys. Res.*, *97*(D5), 6003−6010.

Hoell, J. M., D. D. Davis, S. C. Liu, R. E. Newell, H. Akimoto, R. J. McNeal, and R. J. Bendura (1997), The Pacific Exploratory Mission-West phase B: February−March, 1994, *J. Geophys. Res.*, *102*(D23), 28,223−28,239.

Jacob, D. J., J. H. Crawford, M. M. Kleb, V. S. Connors, R. J. Bendura, J. L. Raper, G. W. Sachse, J. C. Gille, L. Emmons, and C. L. Heald (2003), Transport and Chemical Evolution over the Pacific (TRACE-P) aircraft mission: Design, execution, and first results, *J. Geophys. Res.*, *108*(D20), 9000, doi:10.1029/2002JD003276.

Jaffe, D., et al. (1999), Transport of Asian air pollution to North America, *Geophys. Res. Lett.*, *26*(6), 711−714.

Jaffe, D., I. McKendry, T. Anderson, and H. Price (2003a), Six 'new' episodes of trans-Pacific transport of air pollutants, *Atmos. Environ.*, *37*, 391−404.

Jaffe, D., H. Price, D. Parrish, A. Goldstein, and J. Harris (2003b), Increasing background ozone during spring on the west coast of North America, *Geophys. Res. Lett.*, *30*(12), 1613, doi:10.1029/2003GL017024.

Madronich, S., and S. Flocke (1999), The role of solar radiation in atmospheric chemistry, in *Handbook of Environmental Chemistry*, edited by P. Boule, pp. 1−26, Springer-Verlag, New York.

Martin, B. D., H. E. Fuelberg, N. J. Blake, J. H. Crawford, J. A. Logan, D. R. Blake, and G. W. Sachse (2002), Long-range transport of Asian outflow to the equatorial Pacific, *J. Geophys. Res.*, *108*(D2), 8322, doi:10.1029/2001JD001418. [printed *108*(D2), 2003]

McKeen, S. A., and S. C. Liu (1993), Hydrocarbon ratios and photochemical history of air masses, *Geophys. Res. Lett.*, *20*(21), 2363−2366.

McKeen, S. A., S. C. Liu, E. Y. Hsie, X. Lin, J. D. Bradshaw, S. Smyth, G. L. Gregory, and D. R. Blake (1996), Hydrocarbon ratios during PEM-WEST A: A model perspective, *J. Geophys. Res.*, *101*(D1), 2087−2109.

Merrill, J., M. Uematsu, and R. Bleck (1989), Meteorological analysis of long-range transport of mineral aerosols over the North Pacific, *J. Geophys. Res.*, *94*(D6), 8584−8598.

Moore, K. G., II, A. D. Clarke, V. N. Kapustin, and S. G. Howell (2003), Long-range transport of continental plumes over the Pacific Basin: Aerosol physiochemistry and optical properties during PEM-Tropics A and B, *J. Geophys. Res.*, *108*(D2), 8236, doi:10.1029/ 2001JD001451.

Perry, K. D., T. A. Cahill, R. C. Schnell, and J. M. Harris (1999), Long-range transport of anthropogenic aerosols to the National Oceanic and Atmospheric Administration baseline station at Mauna Loa Observatory, Hawaii, *J. Geophys. Res.*, *104*(D15), 18,521–18,533.

Prospero, J., and D. Savoie (2003), Long-tern record of nss-sulfate and nitrate in aerosols on Midway Island, 1981–2000: Evidence of increased (now decreasing?) anthropogenic emissions from Asia, *J. Geophys. Res.*, *108*(D1), 4019, doi:10.1029/2001JD001524.

Sandholm, S. T., et al. (1992), Summertime tropospheric observations related to N_xO_y distributions and partitioning over Alaska: Arctic boundary layer expedition 3A, *J. Geophys. Res.*, *97*(D15), 16,481–16,509.

Sandholm, S., et al. (1994), Summertime partitioning and budget of NO_y compounds in the troposphere over Alaska and Canada: Arctic boundary layer expedition 3B, *J. Geophys. Res.*, *99*(D1), 1837–1861.

Sandu, A., J. G. Verwer, M. Van Loon, G. R. Carmichael, F. A. Potra, D. Dabdub, and J. H. Seinfeld (1997), Benchmarking stiff ODE solvers for atmospheric chemistry problems-I. Implicit vs explicit, *Atmos. Environ.*, *31*(19), 3151–3166.

Shaw, G. (1980), Transport of Asian desert aerosol to the Hawaiian Islands, *J. Appl. Meteorol.*, *19*, 1254–1259.

Smyth, S., et al. (1996), Comparison of free tropospheric western Pacific air mass classification schemes for the PEM-West A experiment, *J. Geophys. Res.*, *101*(D1), 1743–1762.

Steding, D. J., and A. R. Flegal (2002), Mercury concentrations in coastal California precipitation: Evidence of local and trans-Pacific fluxes of mercury to North America, *J. Geophys. Res.*, *107*(D24), 4764, doi:10.1029/2002JD002081.

Streets, D. G., et al. (2003), An inventory of gaseous and primary aerosol emissions in Asia in the year 2000, *J. Geophys. Res.*, *108*(D21), 8809, doi:10.1029/2002JD003093.

Thornhill, K. L., B. E. Anderson, J. D. W. Barrick, D. R. Bagwell, R. Friesen, and D. H. Lenschow (2003), Air motion intercomparison flights during Transport and Chemical Evolution in the Pacific (TRACE-P)/ACE-ASIA, *J. Geophys. Res.*, *108*(D20), 9001, doi:10.1029/2002JD003108.

Thornton, D. C., A. R. Bandy, B. W. Blomquist, D. D. Davis, and R. W. Talbot (1996), Sulfur dioxide as a source of condensation nuclei in the upper troposphere of the Pacific Ocean, *J. Geophys. Res.*, *101*(D1), 1883–1890.

Thornton, D. C., A. R. Bandy, B. Blomquist, R. Talbot, and J. Dibb (1997), Transport of sulfur dioxide from the Asian Pacific Rim to the North Pacific troposphere, *J. Geophys. Res.*, *102*(D23), 28,489–28,499.

Thornton, D. C., A. R. Bandy, F. H. Tu, B. Blomquist, G. Mitchell, W. Nadler, and D. Lenschow (2002), Fast airborne sulfur dioxide measurements by Atmospheric Pressure Ionization Mass Spectrometry (APIMS), *J. Geophys. Res.*, *107*(D22), 4632, doi:10.1029/2002JD002289.

Tu, F. H., D. C. Thornton, A. R. Bandy, M. S. Kim, G. Carmichael, Y. H. Tang, L. Thornhill, and G. Sachse (2003), Dynamics and transport of sulfur dioxide over the Yellow Sea during TRACE-P, *J. Geophys. Res.*, *108*(D20), 8790, doi:10.1029/2002JD003227.

Uno, I., et al. (2003), Regional chemical weather forecasting system CFORS: Model descriptions and analysis of surface observations at Japanese island stations during the ACE-Asia experiment, *J. Geophys. Res.*, *108*(D23), 8636, doi:10.1029/2002JD003252.

Wilkening, K. E., L. A. Barrie, and M. Engle (2000), Atmospheric science: Trans-Pacific air pollution, *Science*, *290*(5489), 65–67.

Xiao, H., G. R. Carmichael, J. Durchenwald, D. Thornton, and A. Bandy (1997), Long-Range transport of SO_x and dust in east Asia during the PEM-B experiment, *J. Geophys. Res.*, *102*(D23), 28,589–28,612.

————————————

A. R. Bandy, D. C. Thornton, and F. H. Tu, Department of Chemistry, Drexel University, 3141 Chestnut Street, Philadelphia, PA 19104, USA. (dct@drexel.edu)

D. R. Blake, Department of Chemistry, University of California, Irvine, CA 92697-2025, USA.

G. R. Carmichael and Y. Tang, Center for Global and Regional Environmental Research, University of Iowa, Iowa City, IA 52242-1000, USA.

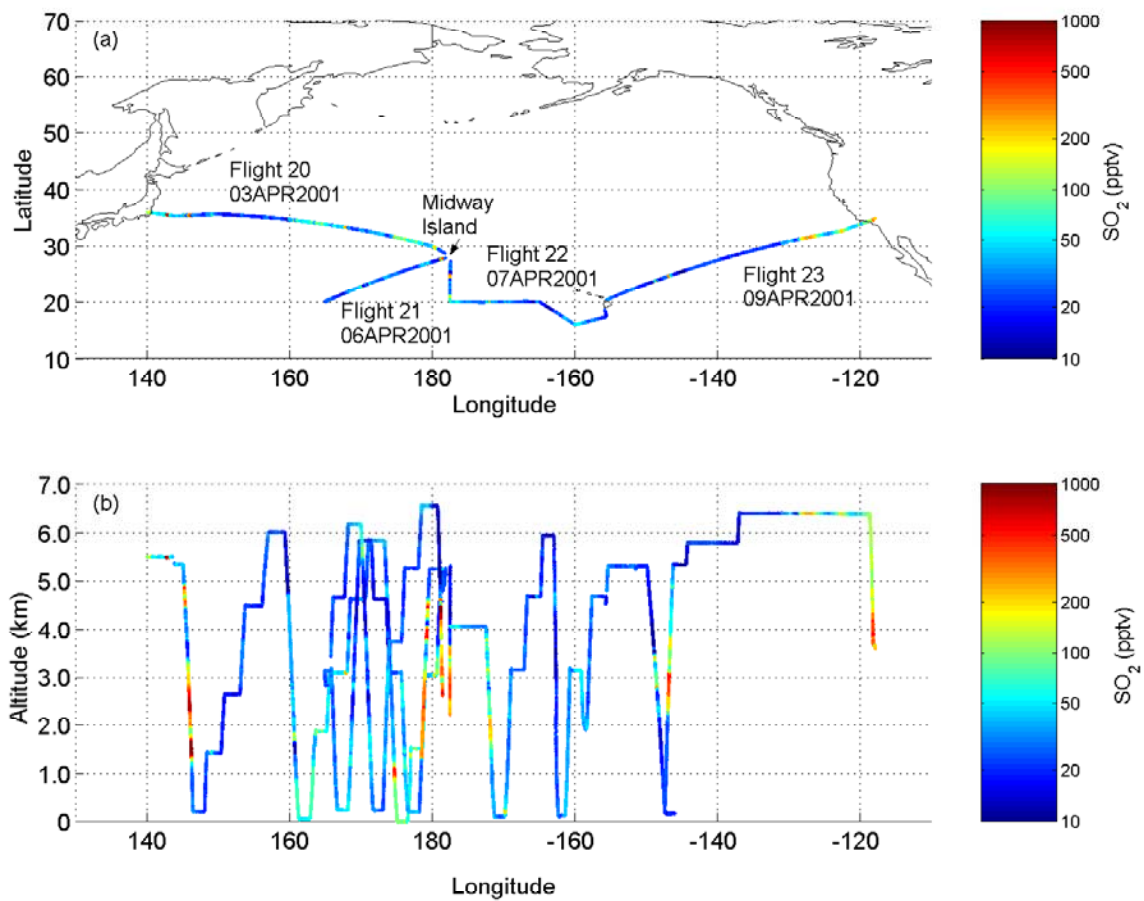G. W. Sachse and K. L. Thornhill, NASA Langley Research Center, Hampton, Virginia 23681-2199, USA.

Figure 1. The SO₂ distributions along the trans-Pacific flight tracks during TRACE-P: (a) flight tracks and (b) altitude profiles. Note the highly varied SO₂ concentrations near Midway Island between 1 and 5 km.
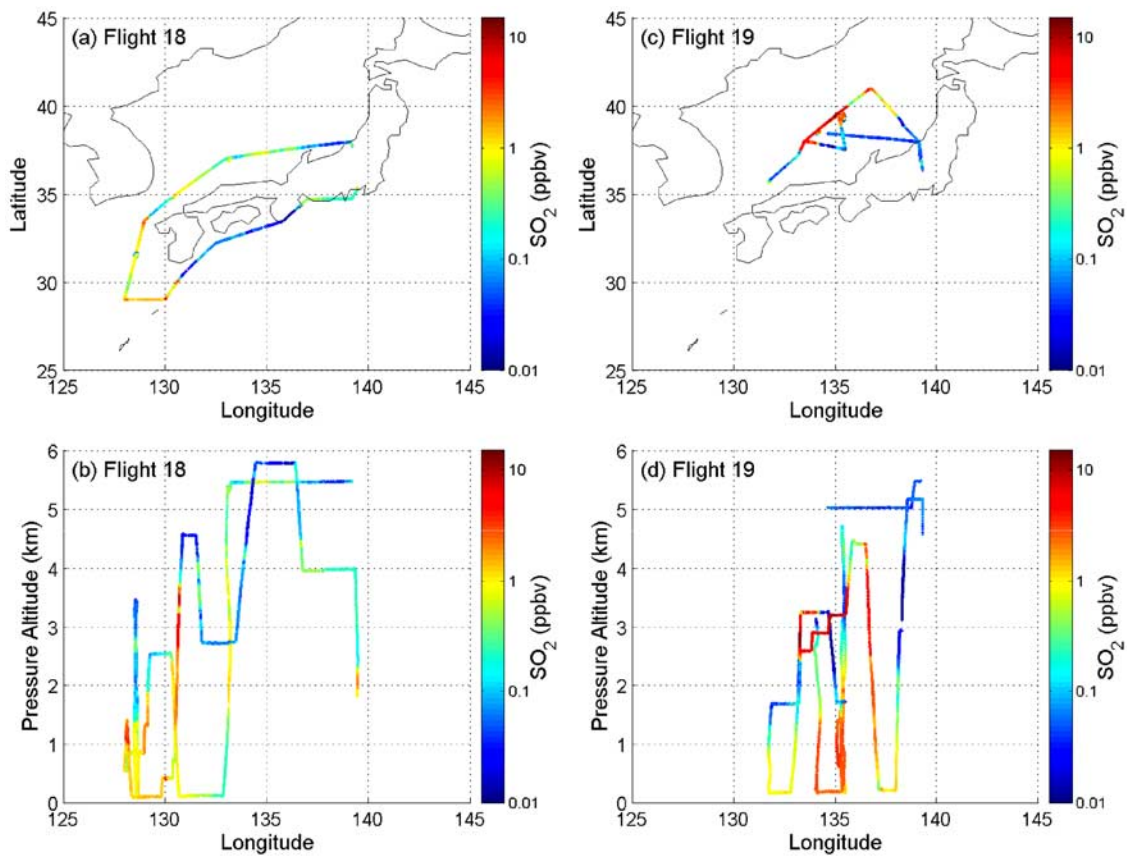
Figure 8. The SO₂ distributions along the tracks for (a, b) flight 18 and (c, d) flight 19. Note the major SO₂ outflow was between 1 and 5 km.